Tribology International 72 (2014) 31–34

Contents lists available at ScienceDirect

Tribology International

journal homepage: www.elsevier.com/locate/triboint

Analysis of static friction and elastic forces in a nanowire bent on a flat surface: A comparative study

Mikk Antsov [a,b,*], Leonid Dorogin [a,b], Sergei Vlassov [a,b], Boris Polyakov [a,c], Mikk Vahtrus [a,b], Karine Mougin [d], Rünno Lõhmus [a,b], Ilmar Kink [a,b]

[a] Institute of Physics, University of Tartu, Estonia, Riia 142, 51014 Tartu, Estonia
[b] Estonian Nanotechnology Competence Centre, Riia 142, 51014 Tartu, Estonia
[c] Institute of Solid State Physics, University of Latvia, Latvia
[d] Institut de Science des Matériaux de Mulhouse, 15 rue Jean Starcky, 68057 Mulhouse, France

ARTICLE INFO

Article history:
Received 18 September 2013
Received in revised form
5 December 2013
Accepted 8 December 2013
Available online 17 December 2013

Keywords:
Nanomanipulation
ZnO nanowire
Static friction
Elasticity

ABSTRACT

ZnO nanowires bent to a complex shape and held in place by static friction force from supporting flat surface are investigated experimentally and theoretically. The complex shapes are obtained by bending the nanowires inside a scanning electron microscope with a sharp tip attached to a nanopositioner. Several methods previously described in the literature are applied along with author's original method to calculate the distributed friction force and stored elastic energy in the nanowires from the bending profile. This comparative study evidences the importance of the usage of appropriate models for accurate analysis of the nanowires profile. It is demonstrated that incomplete models can lead up to an order of magnitude error in the calculated friction force for complex profiles.

1. Introduction

Nanowires (NWs) are known to have unique mechanical [1], optical [2] and electrical [3] properties in comparison to the bulk material and have a number of promising applications in nanoscale mechanics [4], electronics [5] and piezotronics [6]. The progress in miniaturisation and improving the efficiency of micro- and nano-electromechanical systems (MEMS, NEMS) demands accurate modelling of nanoscale phenomena [7]. In particular, adhesion and friction are crucial parameters for the operation of NEMS. Considering that fabrication of NW-based electromechanical devices requires precise control over positioning and subsequent behaviour of the NWs, as well as the fact that friction and adhesion can cause failures of NEMS, it is evident, that deeper understanding of NW-surface interaction mechanisms is essential from applicative point of view.

Friction between an elastically bent NW and a flat substrate has been studied by several authors using atomic force microscopy (AFM) [8–10]. It was shown that NWs possess enhanced flexibility compared to the bulk [11]. At the same time the NW-substrate adhesion and static friction can be high enough to preserve the NW in the bent state. The equilibrium between elastic and friction forces can be utilised to analyse the distributed friction from the known NW bending profile and NW elastic modulus. Such approach was firstly described by Bordag et al. in [10] and further developed by other authors [8,9,12].

Bordag [10] assumed the most bent state of arc-shaped NW to be circular, which enabled to simply use the maximum curvature of such NW as a basis for the static friction calculation. Strus [9] introduced a method, where an AFM image of a bent CNT was used for determining the static friction and elastic stresses in the framework of the elastic beam theory. Stan [8] used parabolas to fit through a defined region of the NW centreline for the analysis with Strus' equilibrium expressions. The drawbacks of the named methods were the unconsidered boundary conditions and incomplete equilibrium equations.

An elaborated method for modelling the static friction force in the framework of the elastic beam theory was proposed and demonstrated for ZnO NWs on silicon substrate by Dorogin et al. [12,13]. The method benefits from fully satisfied boundary conditions and complete equilibrium equations. Although the applicability of the method was demonstrated on arc-shaped NWs, it is also suitable for more sophisticated profiles. The more complex the bending shape is, the more accurate method has to be applied due to high sensitivity of the equilibrium equations to curvature derivatives. Therefore the importance of proper skeletonization and equilibrium force analysis can be hardly overestimated.

* Corresponding author at: Institute of Physics, University of Tartu, Riia 142, 51014 Tartu, Estonia. Tel.: +372 58164820.
E-mail address: Mikk.Antsov@ut.ee (M. Antsov).

0301-679X/$ - see front matter © 2013 Elsevier Ltd. All rights reserved.
http://dx.doi.org/10.1016/j.triboint.2013.12.010

The aim of the present paper is to revise and compare three above-mentioned methods [8–10] in application to NWs bent to complex shapes and to propose a refined method based on Dorogin's original method [12]. ZnO NWs were deposited onto an oxidised silicon substrate and then bent using an AFM tip attached to a piezo-driven manipulator inside a scanning electron microscope (SEM) chamber like described in [13]. The SEM images of NWs were acquired and used for extracting NW-substrate static friction distribution by four above mentioned methods. The results are compared and analysed. Interpretation of the differences in the obtained quantities is given with a reference to physical and geometrical peculiarities of the problem.

2. Theoretical background: elastic beam theory for 1D nanostructures

Let us consider a prismatic NW elastically bent in a plane under external lateral forces, which may consist of uniformly distributed or point forces. As a result, the NW is kept in equilibrium due to the balance of intrinsic elastic forces and external forces. In this case the common elastic beam theory [14] can be employed to find the equilibrium equations for the NW. They include the force **F** and momentum **M** of the elastic stress defined as integrals of cross-section S at any given point l along the NW axis by components [14]

$$F_i = \int_S \sigma_{i\gamma} n_\gamma dS \tag{1}$$

$$M_i = \int_S e_{i\alpha\beta} r_\alpha \sigma_{\beta\gamma} n_\gamma dS \tag{2}$$

where $\sigma_{\beta\gamma}$ is the component of the stress tensor, η_γ is the component of the normal vector of the elements of the cross-section area dS, r_α is the component of the radius vector from the axial point l and $e_{i\alpha\beta}$ is the unit anti-symmetric tensor. Both the momentum **M** and the elastic force **F** are functions of the coordinate l along the axis of the NW.

For a NW at equilibrium, the equations of the full system between the force **F** and the momentum **M** are as follows:

$$\frac{d\mathbf{F}}{dl} = -\mathbf{f} \tag{3a}$$

$$\frac{d\mathbf{M}}{dl} = \mathbf{F} \times \mathbf{t} \tag{3b}$$

where **f** is the external distributed force per unit length acting on the NW and **t** is the tangent vector of the NW axis.

For the pure bending case of prismatic NWs we obtained the following equations:

$$\mathbf{M} = EI\mathbf{t} \times \frac{d\mathbf{t}}{dl} \tag{4}$$

where E is the Young modulus and I is the area moment of inertia of the NW. Since the NW deformation is in a plane, **M** is always directed out of the plane and Eq. (4) can be rewritten as:

$$M = EI\frac{d\phi}{dl} = EI\kappa \tag{5}$$

where the curvature κ can be defined as $\kappa = d\phi/dl = 1/R$, where φ is the tangent angle along the NW in the point l, and R is the local radius of curvature.

In case of a NW bent on a surface, the distributed static friction force $\mathbf{F}^{st}$ plays the role of an external force: $\mathbf{f} = \mathbf{F}^{st}$. In order to complete the equations of equilibrium, the tangential component of the static friction is assumed to be negligibly small $F_t^{st} = 0$. Solution of the Eqs. (3a), (3b) and (5) with respect to $\mathbf{F}^{st}$ as a function of l was obtained by Strus [9] and then employed by Stan [8]. Independently the solution was obtained by Dorogin [12], which contained an additional term (as can be seen from Table 1). It must be noted that Bordag [10] had deduced the expression for $\mathbf{F}^{st}$ directly from the integrated elastic energy of a circularly bent NW.

3. Experimental

ZnO NWs grown by the vapour transport method (VTM) [15] were chosen for manipulation experiments. NWs obtained by the VTM method have shown well-defined geometrical structure, with well-structured facets [16] and proper mechanical properties for manipulation experiments. The NWs obtained ranged from 10 to 20 μm in length and from 60 to 200 nm in diameter.

The manipulation experiments were conducted inside a SEM (Tescan VEGA II) using a contact AFM cantilever (Nanosensor ATEC-CONT cantilevers $C = 0.2$ N/m) mounted onto a 3-dimensional nanomanipulator (SmarAct SLC-1720-S). The geometry of the cantilever provided tip visibility from the top. The NWs were mechanically transported from the VTM grown substrate by either scraping it with a sharp tip or using cleanroom wipes to pick up the wires by touching the substrate and moving them to a silicon surface. During the transport the NWs were broken into shorter pieces (1–10 μm). More details about the experimental nanomanipulation setup can be found in [13].

A single NW on a silicon surface was manipulated by the following procedure. The substrate with the deposited NWs was inspected in SEM and a single NW of appropriate aspect ratio in the range from 30 to 60 was selected. These NWs can be bent into complex shapes more easily. For lower aspect ratios the elastic forces in a bent NW tend to overcome the static friction force and arc-shapes can be obtained. Proper NW was chosen and gradually bent with the AFM tip on the surface of the substrate. After retraction of the tip the residual bent shape of the NW was determined by the balance between the elastic and the interfacial

Table 1
Analytical expressions and calculated values of static friction distribution between the complexly bent NW and substrate (for description see text).

Authors	Static friction between the NW and substrate			
	Analytical expression	Average value (nN/nm)	Maximal value (nN/nm)	Magnitude of the total force (nN)
Bordag et al. [10][a]	$F_n^{st} = (EI/2)\kappa^3$	0.024	0.1	0.004
Strus et al. [9]	$F_n^{st} = EI(d^2\kappa/dl^2)$	0.21	0.49	29
Stan et al. [8][b]	$F_n^{st} = -EI\frac{24A^3(16A^2x^2+16ABx+4B^2-1)}{(4A^2x^2+4ABx+B^2+1)^{9/2}}$	0.19	1.4	9.5
Dorogin et al. [12]	$F_n^{st} = EI(d^2\kappa/dl^2)+(\kappa^3/2)$	0.20	0.38	0

[a] Modified Bordag using our skeleton as a basis.
[b] x is the coordinate in the plane of the SEM image.

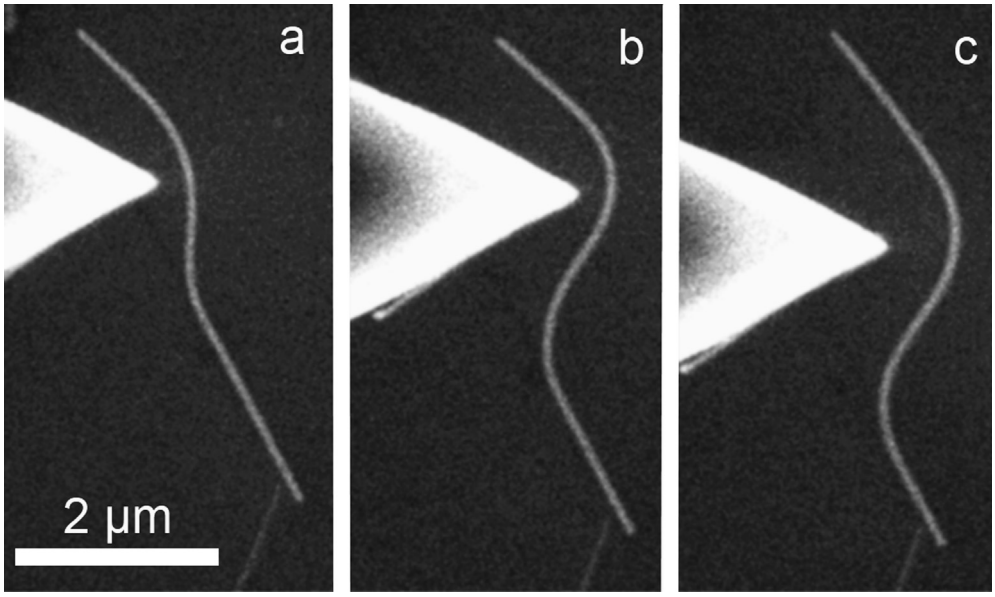

Fig. 1. Continuous set of SEM images of ZnO NW bent into S-shape by AFM tip. The NW diameter is 90 nm and length is 5.5 μm.

forces. The procedure was repeated many times with different NWs and different shapes were obtained.

A single S-shaped NW with appropriate aspect ratio was chosen (Fig. 1b) and different methods for calculation of the distributed friction force were applied and compared.

4. Results and discussion

Firstly it is necessary to know the exact geometry, size and elastic modulus of the NWs for the application of the elastic beam theory and the determination of the distributed friction force in all considered methods. These properties strongly influence the interfacial forces acting between the surface and the NW and thus affect the mechanical behaviour of the NWs. The cross-section of ZnO NWs used in our experiment is assumed to be hexagonal [17]. Young's modulus of 58 GPa was used for the friction calculation, as measured for the same type of ZnO NWs in our earlier work [13].

The second step is a skeletonization, i.e. extracting the centreline and subsequently the local curvature distribution function. Different authors used different skeletonization procedures. Stan [8] and Strus [9] both used the software DataThief, although the final skeleton obtained for the friction analysis was slightly different. Strus [9] used the raw DataThief data and smoothened it with three- and five-point running mean average filters. Stan provided no information about smoothening and therefore we assumed that the raw skeleton was used. Stan applied parabola-fitting, where a parabola in the form $y=Ax^2+Bx+C$ was fitted at each point along the NW skeleton comprising of six adjacent points (three at each side).

The skeletonization proposed by Dorogin et al. in [12] is distinctive in the usage of specially defined polynomials for the curvature distribution. It enabled to comply with the boundary conditions of the free ends of the NW already at the stage of skeletonization. Another advantage is the direct fitting and the interpolation of the centreline without additional filtering.

Bordag in his original paper [10] did not use any skeletonization algorithm. Instead a circle was fitted to the image of the NW to find the single value of the radius of curvature in the most bent part of the NW for determination of the maximum value of static friction. In the current paper the curvature function based on Dorogin's method was used for Bordag's static friction calculation

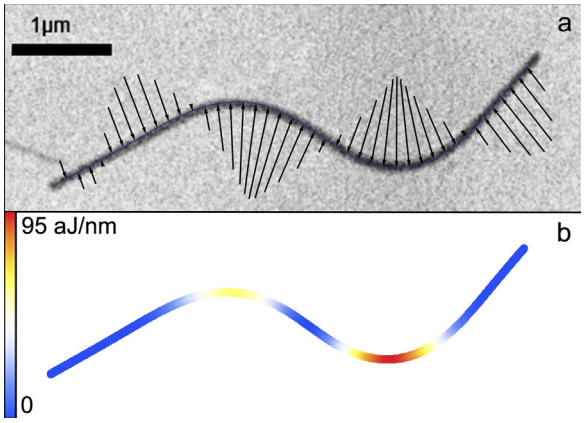

Fig. 2. Static friction (a). Elastic energy (b). The total calculated elastic energy stored in the NW is 0.14 pJ.

to obtain the friction force values not only in the most bent state, but at each point of the NW.

At the third (final) step the static friction force distribution, the elastic energy distribution and the total elastic energy can be calculated if the curvature distribution is known. The analytical expressions for the friction distribution are summarised in Table 1. Bordag [10], on the basis of the fact that an elastically bent beam stores a certain amount of elastic energy, extracted the restoring force of a circularly bent beam and identified it as the static friction force.

Strus [9] and Stan [8] both calculated the friction force from the equilibrium equations of an elastic beam without taking the boundary conditions into account. Moreover, as it can be seen from Strus' expression, only the 2nd derivative term is present. Stan used the same solution for the friction distribution, but expressed it in the terms of parabolic coefficients A and B. Due to an algebraic mistake found in [8] the expression was corrected and used henceforth.

Dorogin [12] had employed the equilibrium equations likewise and obtained similar result to Strus' with the additional term proportional to the cube of the curvature.

Let us now consider all described methods applied to a S-shaped NW (see Fig. 2a). The numerical results for the average and maximum

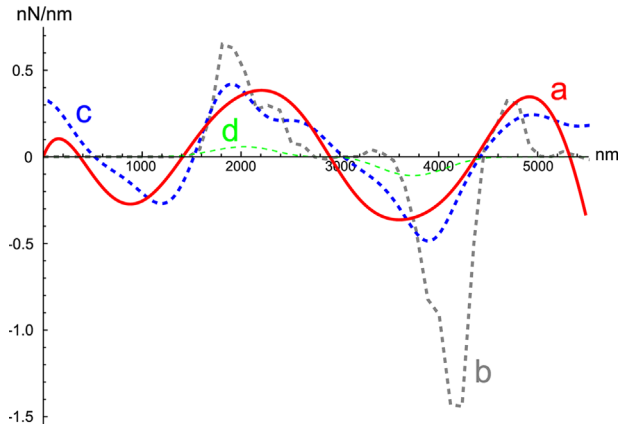

Fig. 3. Calculated static friction force distributions along a selected NW by four different methods: Dorogin's (a), Stan's (b), Strus' (c), and Bordag's (d).

static frictions per unit length and the total static friction force magnitude are presented in Table 1 for all methods. The diagram with the static friction distributions along the NW for all methods is depicted in Fig. 3, whereas Fig. 2 contains the friction and elastic energy distributions from Dorogin's method only.

From Table 1, it is evident that the method proposed by Bordag [10] underestimates the friction force. Stan's method also has certain drawbacks. The centreline acquired with the DataThief software may contain local disturbances if the original image is not smooth enough. Therefore, Stan's result is exposed to high frequency artefacts arising from the higher order derivatives used to calculate the static friction and therefore is more sensitive to small disturbances in the curvature of the NW. Due to the fact that Strus used averaging filters the obtained static friction distribution is relatively smooth compared to the result obtained by Stan.

Moreover, the methods by Bordag, Strus and Stan neglect the role of the free ends of NWs and yield a nonzero magnitude of the total force. This is partly due to the incomplete equilibrium equations used for calculating the friction force and partly due to an error in the skeletonization that leads to the breaking of the boundary conditions. The later problem is elegantly solved in Dorogin's method by application of specially selected polynomials in numerical calculations. The results of Dorogin's algorithm applied to S-shaped ZnO NW are shown in Fig. 2, where the arrows indicate the direction and amplitude of the normal component of the static friction.

5. Conclusions

The shape of an elastically bent NW on a flat substrate results from the competition between the elastic restoring forces within the wire and the friction forces between the wire and the substrate. Thus Young's modulus, cross section, and deformation profile of the NW completely determine the magnitude and distribution of static friction along the wire.

A model for calculation of the distributed static friction force for a NW bent into arbitrary/complex shape and lying on a flat surface was elaborated and compared with the already existing models. Our proposed method benefits from the utilisation of specially selected polynomials exhibiting a higher level of accuracy due to the boundary conditions incorporated at the pre-processing stage and complying with the complete set of the elastic equilibrium equations.

The proposed method along with the other existing methods was applied to a ZnO NW bent to S shape on a silicon wafer. The calculations of the static friction force and distributed elastic energy along the NW demonstrated up to an order of magnitude errors for the complex shaped profiles in the other models. This fact was confirmed by comparison of the total friction force values.

Acknowledgement

This work was supported by the Estonian Science Foundation (Grant JD162), and the European Union through the European Regional Development Fund (Centre of Excellence "Mesosystems: Theory and Applications", TK114). The work was also partly supported by ETF grants 8420 and 9007, the Estonian Nanotechnology Competence Centre (EU29996), ERDF "TRIBOFILM" 3.2.1101.12-0028, "IRGLASS" 3.2.1101.12-0027,"Nano-Com" 3.2.1101.12-0010 and COST Action MP1303.

References

[1] Wu B, Heidelberg A, Boland JJ. Mechanical properties of ultrahigh-strength gold nanowires. Nat Mater 2005;4:525–9.
[2] Hocevar M, Immink G, Verheijen M, Akopian N, Zwiller V, Kouwenhoven L, et al. Growth and optical properties of axial hybrid III–V/silicon nanowires. Nat Commun 2012;3.
[3] Hu1 J, Ouyang M, Yang P, Lieber CM. Controlled growth and electrical properties of heterojunctions of carbon nanotubes and silicon nanowires. Nature 1999;399:48–51.
[4] Fernandez-Regulez M, Sansa M, Serra-Garcia M, Gil-Santos E, Tamayo J, Perez-Murano F, et al. Horizontally patterned Si nanowire growth for nanomechanical devices. Nanotechnology 2013;24:095303.
[5] Ionescu AM. Electronic devices: nanowire transistors made easy. Nat Nanotechnol 2010;5:178–9.
[6] Wang ZL. Piezopotential gated nanowire devices: piezotronics and piezophototronics. Nano Today 2010;5:540–52.
[7] Samuelson L. Self-forming nanoscale devices. Mater Today 2003;6:22–31.
[8] Stan G, Krylyuk S, Davydov AV, Cook RF. Bending manipulation and measurements of fracture strength of silicon and oxidized silicon nanowires by atomic force microscopy. J Mater Res 2012;27:562–70.
[9] Strus MC, Lahiji RR, Ares P, López V, Raman A, Reifenberger R. Strain energy and lateral friction force distributions of carbon nanotubes manipulated into shapes by atomic force microscopy. Nanotechnology 2009;20:385709.
[10] Bordag M, Ribayrol A, Conache G, Fröberg L, Gray S, Samuelson L, et al. Shear stress measurements on InAs nanowires by AFM manipulation. Small 2007;3:1398–401.
[11] Polyakov B, Dorogin LM, Vlassov S, Kink I, Lõhmus A, Romanov AE, et al. Real-time measurements of sliding friction and elastic properties of ZnO nanowires inside a scanning electron microscope. Solid State Commun 2011;151:1244–7.
[12] Dorogin LM, Polyakov B, Petruhins A, Vlassov S, Romanov AE. Modeling of kinetic and static friction between an elastically bent nanowire and a flat surface. J Mater Res 2011;27:580.
[13] Dorogin LM, Vlassov S, Polyakov B, Antsov M, Lõhmus R, Kink I, et al. Real-time manipulation of ZnO nanowires on a flat surface employed for tribological measurements: experimental methods and modeling. Phys Status Solidi B 2012:1–13.
[14] Landau L, Lifshitz E. Theory of elasticity. Oxford: Butterworth–Heinemann; 1986.
[15] Huang MH, Wu Y, Feick H, Tran N, Weber E, Yang P. Catalytic growth of zinc oxide nanowires by vapor transport. Adv Mater 2001;13:113–6.
[16] Gao PX, Ding Y, Wang ZL. Crystallographic orientation-aligned ZnO nanorods grown by a tin catalyst. Nano Lett 2003;9:1315–20.
[17] Zhu Z, Chen TL, Gu Y, Warren J, Osgood RM. Zinc oxide nanowires grown by vapor-phase transport using selected metal catalysts: a comparative study. Chem Mater 2005;17:4227–34.